Soumis pour publication au
Journal of Solid State Chemistry

LANTHANIDE BOROGERMANATES $LnBGeO_5$: SYNTHESIS AND STRUCTURAL STUDY BY X-RAY DIFFRACTOMETRY AND VIBRATIONAL SPECTROSCOPY.

A. RULMONT and P. TARTE.

University of Liège, Institute of Chemistry
B-4000 Sart Tilman par Liège 1.
BELGIUM.

ABSTRACT.

$LnBGeO_5$ borogermanates have been synthesized by solid state reaction and investigated by powder x-ray diffractometry, infrared and Raman spectroscopy.
A hexagonal, stillwellite-like phase, is obtained for Ln= La, Pr and Nd (low-temperature phase). Smaller cations (Nd to Er, and Y) lead to a monoclinic phase, Z = 4, with a = 9.80-10.03, b = 7.42-7.60, c = 4.79-4.96 Å, and β = 91°14'-91°54', depending on the ionic radius of the rare earth. For the smallest lanthanides (Tm, Yb, Lu), no monoclinic phase is obtained : $Ln_2Ge_2O_7$ is eventually formed, with a total loss of B_2O_3.
The vibrational spectrum of the monoclinic phase points to some analogies with the stillwellite structure, namely a tetrahedral coordination of boron, and an ordered distribution of the BO_4 and GeO_4 tetrahedra.

INTRODUCTION.

So far, two borogermanates only have been reported and structurally investigated : $LiBGeO_4$, structurally similar to $BAsO_4$ (1,2), and the complex compound $Ca_3Er_3Ge_2BO_{13}$ with a sulphohalite-like structure (3).
All attempts to synthesize borogermanates $M^IBGe_2O_6$ (similar to the pollucite-like borosilicates $M^IBSi_2O_6$) met no success (4).
Among the number of well-known borosilicates, the lanthanide compounds $LnBSiO_5$ with a stillwellite structure have recently received some attention in connection with the hydrothermal cristallization of a radioactive waste storage glass (5).
We have accordingly investigated the possible existence of the corresponding borogermanates.

EXPERIMENTAL.

$LnBGeO_5$ borogermanates have been synthesized by solid state reaction between stoichiometric quantities of Ln_2O_3 (or commercially available oxides such as CeO_2, Tb_4O_7 and Pr_6O_{11}) of 99.9 % purity, H_3BO_3 and GeO_2 (analytical purity). Some syntheses were also carried out with a 5 to 10 % (mol) excess of H_3BO_3.
The mixture is well ground and mixed under petroleum ether, and progressively heated in covered platinum crucibles up to 850 °C. After 1 day at this temperature, the mixture is reground, and the temperature is increased by steps of 50 °C (up to a maximum of 1100 °C) with intervening mixing and grinding.
The progress of the reaction is observed by IR spectroscopy and x-ray diffraction, and the thermal treatment is resumed so long as modifications are observed in the spectra.
The x-ray powder diagrams have been registered with a CGR diffractometer (Co Kα monochromatized radiation). The IR spectra have been registered by the conventional pressed disc technique (Beckman 4250 spectrophotometer and KBr discs in the 2000-300 cm^{-1} region ; Polytec FIR 30 interferometer and polyethylene discs in the 350-30 cm^{-1} region). The Raman spectra were obtained with a CODERG double monochromator equipped with a Spectra-Physics Ar^+ laser (5145 Å green line, 200 mW, spectral slit width of about 1.5 cm^{-1} for most spectra, increased to 3 cm^{-1} for the weak bands).

RESULTS.

X-ray diffraction.

For Ln = La and Pr, the x-ray powder diagram is very similar to that of stillwellite $LaBSiO_5$ (ASTM cards N° 19-650, 25-1447, 26-349), and is easily indexed by comparison (Table 1).
The assignment to a stillwellite structure is supported by the very good agreement between observed and calculated d values.
The behavior of the Nd_2O_3 - GeO_2-B_2O_3 system is more complicated. In the temperature range just sufficient to start the reaction (850-900 °C), both IR and x-ray data point to the formation of a stillwellite phase, but the reaction is too sluggish to go to completion.

At the higher temperatures necessary to have a complete reaction, the stillwellite phase disappears and is replaced by a new single phase, which is also obtained directly (without the intermediate formation of a stillwellite) with the smaller cations Sm to Er, and Y. However, the reaction, which is easy for Sm, Eu and Gd, becomes more and more difficult when the ionic radius of the cation decreases, and the compounds with the small cations Ho, Er and Y could not be obtained completely free from the corresponding pyrogermanate $Ln_2Ge_2O_7$, which is formed by the loss of B_2O_3. This could not be completely avoided by the addition of a small excess of H_3BO_3.
Finally, no definite borogermanate could be obtained with the smallest cations Tm, Yb and Lu : we obtained a mixture of unidentified phases which is progressively transformed into $Ln_2Ge_2O_7$ with a total loss of B_2O_3.
The x-ray powder diagram of the new phase (Nd to Er) has been indexed with the help of the Visser Program (6) : all reflections are satisfactorily accounted for by a monoclinic cell (Table 2) ; the refinement of the unit cell parameters was carried out by a least-squares program. The measured density of the Nd compound is 5.40 $g.cm^{-3}$, against a calculated value of 5.417 $g.cm^{-3}$ for Z = 4.
All data are collected in Table 3, which also includes the values of M_{20} (7) and F_N (8), calculated for the Co Kα radiation.
Most of the parameters exhibit a nearly linear variation with the ionic radius of the rare earth (Fig. 1).

Vibrational spectra.

In view of the complexity of the spectra, we shall restrict the discussion to some essential features.

Hexagonal (stillwellite) phases.

We can point out the following facts :
i. All the observed frequencies are located below 1100 cm^{-1} (Fig. 2 and 3). The coordination of boron is thus tetrahedral, in agreement with the proposed stillwellite structure of these phases.

ii. The strong IR bands of the 1000-900 cm^{-1} region exhibit fairly large ^{10}B-^{n}B isotopic shifts (15 to 28 cm^{-1} : table 4) and are thus predominantly stretching, antisymmetric motions of BO_4 tetrahedra.
Bands with a similar isotopic behavior are observed at somewhat higher frequencies (between 1040 and 980 cm^{-1}) in the spectrum of the corresponding silicate $LaBSiO_5$ (Fig. 2).
This frequency increase may be due, either to the smaller unit cell parameters of the silicate, or to interactions between BO_4 and SiO_4 vibrations, or both.
These bands are missing in the Raman spectrum but, even if they are allowed, they are expected to be weak because of their antisymmetric character and of the low polarizability of the BO_4 group.
Conversely, the strong bands observed in the 900-800 (Ra) and 800-700 (IR) cm^{-1} region exhibit no or small ^{10}B-^{n}B isotopic shifts.
Similar bands (by their intensity and their isotopic behavior) are observed at fairly higher frequencies in the spectrum of the silicate.
The IR bands are thus assigned to vibrations which are essentially stretching motions of the GeO_4 (SiO_4) tetrahedra with a small contribution from the BO_4 tetrahedra, as indicated by the small (but quite reproducible) ^{10}B-^{n}B isotopic shifts.
The Raman peaks may be assigned partly to symmetric BO_4 vibrations, or to GeO_4 vibrations.

iii. Only tentative assignments can be proposed for the lower frequency bands. The stillwellite structure is characterized by the existence of chains of BO_4 tetrahedre (10). The weak bands of the 700-500 cm^{-1} region may be assigned to chain vibrations which have a mixed stretching-bending character.
The stronger bands of the 450-300 cm^{-1} region are probably bending vibrations of the GeO_4 tetrahedra. This is supported by the existence of similar bands in the 550-450 cm^{-1} region of the spectrum of the silicate.
The lower frequency bands correspond to lattice modes, but we have been unable to find clear-cut mass effects which would identify the translations of the cation (La or Pr).

iv. There are some IR-Ra coincidences, in agreement with the lack of a centre of symmetry.

Monoclinic phases. We shall consider only those spectral features which can give structural information.
The high-frequency part of the IR spectrum is somewhat similar to that of the stillwellite phase, with a first group of strong bands (the higher-frequency ones) characterized by large ^{10}B-^{n}B isotopic shifts, and a second group (800-700 cm^{-1}) with small to negligible isotopic shifts (Table 5 and Fig. 4).
The highest-frequency band is located near 1100 cm^{-1}, and it can be immediately inferred that, here also, the coordination of boron is tetrahedral.
The sharpness of the bands (particularly striking in the low frequency part of the Raman spectrum) implies an ordered distribution of B and Ge over the tetrahedral sites.
Finally, the existence of several IR-Ra coincidences suggests the lack of a centre of symmetry (although the possibility of accidental coincidences cannot be totally ignored).

DISCUSSION.

COMPOUNDS WITH THE STILLWELLITE STRUCTURE.

Besides the mineral itself, which has a more or less complex composition (Ln, Ca) (Si, Al, P) B $(O, OH, F)_5$ (11), the stillwellite structure is now represented by four chemical families :

- The borosilicates $LnBSiO_5$ (Ln = La, Ce, Pr, Nd, Sm) obtained by hydrothermal synthesis (12).

- The borogermanates $LnBGeO_5$ (Ln = La, Pr, Nd) prepared by solid state reaction and described in this paper. Since the stillwellite type Nd compound can be obtained only at relatively low temperature, it is reasonable to suppose that this structural family can be extended towards smaller rare earths by hydrothermal synthesis. We intend to carry out research in this direction.

- The borophosphates $M^{II}BPO_5$, with M^{II} = Ca, Sr, Ba (13) or Pb (14).
- The corresponding boroarsenates $M^{II}BAsO_5$ (13, 14).

In his study of boro-phosphates and -arsenates (13), Bauer did not realize the structural analogy of these compounds with stillwellite and, for some unknown reason, he proposed for the c axis a value which is twice the value observed in the stillwellite family. We have shown (14) that this leads systematically to even values of ℓ and that, consequently, the c axis must be halved. In this way, the indexed powder diagram is very similar to that of stillwellite.
So far, the stillwellite structure is restricted to borocompounds in which boron is associated to a high-valency element with a rather small ionic radius (Si, Ge, P, As), and to another element with a large ionic radius and a moderate valency.

THE MONOCLINIC PHASE.

The very structure of this phase is unknown, but the existing structural information is in agreement with solid state chemistry predictions :

- The four-fold coordination of boron may be related to the presence of the high-valency cation Ge.

- The ordered distribution of the BO_4 and GeO_4 tetrahedra is probably imposed by the large difference between the sizes of the BO_4 and GeO_4 groups, which precludes a statistical distribution of B and Ge over equivalent tetrahedral sites. This is a first confirmation of our prediction that, whenever borogermanates do exist, their structure must be characterized, either by different coordinations of B and Ge, or by an ordered distribution of BO_4 and GeO_4 tetrahedra (2). By the way, this prediction is also verified by the structure of the complex borogermanate $Ca_3Er_3Ge_2BO_{13}$ (3).

So far, we don't know to what extent the structure of the monoclinic phase is different from that of stillwellite. The molecular volumes of hexagonal La and $PrBGeO_5$ lead by extrapolation to an approximate value of 93.3 $Å^3$ for hexagonal $NdBGeO_5$, to be compared with the 94.35 $Å^3$ figure for the monoclinic phase of the same compound. The fact that both structures exist for the Nd compound with similar values of the molecular

volume suggests that the structures are not too different. A chain arrangement of the BO_4 tetrahedra (as in stillwellite) cannot be excluded. The possible existence of the corresponding silicates is still to be investigated. An attempt to synthesize $GdBSiO_5$ by solid state reaction was unsuccessful, but more systematic work, including the use of hydrothermal reactions, is needed.

ACKNOWLEGDEMENTS.

The authors gratefully acknowledge the financial support of the Fonds National de la Recherche Scientifique.

REFERENCES.

(1) J. LIEBERTZ and S. STAEHR, Z. Kristallogr. 155, 115 (1981).
(2) A. RULMONT, P. TARTE and J.M. WINAND, J. Mater. Sci. Letters, 6, 659 (1987).
(3) J. CHENAVAS, I.E. GREY, J.C. GUITEL, J.C. JOUBERT, M. MAREZIO, J.P. REMEIKA and A.S. COOPER, Acta Crystallogr. B 37, 1343 (1981).
(4) D.W. RICHERSON and F.A. HUMMEL, J. Amer. Ceram. Soc. 55, 269 (1972).
(5) D. SAVAGE, J.E.ROBBINS and R.J. MERRIMAN, Mineral. Mag. 49, 195 (1985).
(6)J.M. VISSER, J. Appl. Crystallogr. 2, 89 (1969).
(7) P.M. DE WOLFF, J. Applied. Crystallogr. 1, 108 (1968).
(8) G.S. SMITH and R.L. SNYDER, J. Appl. Crystallogr. 12, 60 (1979).
(9) R.D. SHANNON, Acta Crystallogr. A 32, 751 (1976).
(10) A.A. VORONKOV and Yu.A. PYATENKO, Soviet Physics, Crystallography, 12, 214 (1967) (English Translation).
(11) P. GAY, Mineral. Mag. 31, 455 (1957).
(12) I. Ya. NEKRASOV and R.A. NEKRASOVA, Dokl. Akad. Nauk SSSR (Mineral.) 201, 1202 (1971).
(13) H. BAUER, Z. Anorg. Allg. Chemie 337, 183 (1965)
345, 225 (1966).
(14) P. TARTE and U. DE WISPELAERE-SCHROEDER, C.R. Acad. Sci. Paris, II-295, 351 (1982).

TABLE 1.

Indexed x-ray powder diagram of $LaBGeO_5$ and unit cell parameters of hexagonal compounds

I	h k l	d_{obs}	d_{calc}
7	1 0 0	6.0590	6.0555
14	1 0 1	4.5463	4.5407
88	1 1 0	3.4995	3.4962
6	1 1 1	3.1149	3.1153
65	2 0 0	3.0278	3.0278
100	1 0 2	2.9849	2.9855
4	2 0 1	2.7703	2.7702
18	1 1 2	2.4488	2.4490
25	2 1 0	2.2880	2.2888
	0 0 3		2.2877
26	2 0 2	2.2708	2.2704
18	2 1 1	2.1717	2.1712
2	1 0 3	2.1404	2.1401
3	3 0 0	2.0174	2.0185
3	3 0 1	1.9372	1.9365
68	2 1 2	1.9035	1.9041
17	3 0 2	1.7400	1.7398
22	3 1 0	1.6797	1.6795
12	1 0 4	1.6506	1.6508
12	2 2 2	1.5578	1.5576
5	1 1 4	1.5403	1.5403
5	3 1 2	1.5093	1.5085
6	2 0 4	1.4925	1.4928

$LaBGeO_5$: hexagonal a = 6.9923(8) c = 6.8631(17) Å
V = 290.60(8) A^{o3}
F_N = 45.30 (0.014,25) M_{14} = 75.6

$PrBGeO_5$: hexagonal a = 6.9352(11) c = 6.8080(20) Å
V = 283.57 (10) A^{o3}
F_N = 38.70 (0.014,25) M_{12} = 72.8

F_N has been calculated for the CoKα radiation, taking into account the extinction rules of the $P3_1$ space group of stillwellite.

TABLE 2.

Indexed x-ray powder diagram of $EuBGeO_5$.

I	h k l	d_{obs}	d_{calc}
30	1 1 0	6.0136	6.0115
9	2 0 0	5.0013	4.9959
17	$\bar{1}$ 1 1	3.8260	3.8239
30	1 1 1	3.7605	3.7596
30	$\bar{2}$ 0 1	3.5486	3.5443
29	1 2 0	3.5250	3.5215
67	2 0 1	3.4427	3.4437
100	$\bar{2}$ 1 1	3.2083	3.2065
70	2 1 1	3.1331	3.1315
8	3 1 0	3.0459	3.0457
8	2 2 0	3.0033	3.0057
55	0 2 1	2.9816	2.9812
82	$\bar{1}$ 2 1	2.8719	2.8706
67	1 2 1	2.8447	2.8431
37	$\bar{3}$ 1 1	2.6158	2.6157
33	3 1 1	2.5547	2.5546
5	4 0 0	2.4977	2.4980
25	0 0 2	2.4423	2.4427
43	4 1 0	2.3700	2.3708
10	$\bar{1}$ 1 2	2.2749	2.2768
42	2 3 0 $\bar{3}$ 2 1	2.2407	2.2419 2.2410
8	4 0 1	2.1998	2.1986
5	0 2 2	2.0492	2.0489
12	$\bar{1}$ 2 2	2.0167	2.0167
11	1 2 2 $\bar{3}$ 0 2	1.9977	1.9976 1.9974
15	5 1 0 $\bar{4}$ 2 1 $\bar{3}$ 1 2	1.9317	1.9314 1.9314 1.9305
2	$\bar{2}$ 2 2	1.9116	1.9119
14	3 1 2 0 4 0 2 2 2	1.8804	1.8815 1.8815 1.8798
4	1 4 0	1.8498	1.8490
6	$\bar{5}$ 1 1	1.8130	1.8135
2	5 1 1	1.7789	1.7793
2	4 3 0	1.7700	1.7701
20	0 4 1	1.7553	1.7558
11	$\bar{4}$ 1 2	1.7244	1.7250
19	$\bar{4}$ 3 1	1.6756	1.6752

TABLE 3.

Unit cell parameters of the monoclinic phases.

Ln	a	b	c	β	M_{20}	F_N*
Nd	10.0292(28)	7.5957(13)	4.9568(12)	91°53.9'(1.5')	21.8	18 (0.013, 84)
Sm	10.0032(22)	7.5446(24)	4.9065(11)	91°46.9'(0.7')	18.4	15.2(0.016,100)
Eu	9.9960(10)	7.5260(14)	4.8874(9)	91°39.0'(0.6')	26.4	19.4(0.015.126)
Gd	9.9897(20)	7.5103(14)	4.8741(8)	91°34.7'(1')	18.1	16.2(0.018,111)
Tb	9.9620(20)	7.4903(20)	4.8433(12)	91°30.1'(1')	26.5	14.5(0.022,105)
Dy	9.9443(14)	7.4698(16)	4.8295(8)	91°24.2'(0.8')	23.3	20.2(0.017,110)
Ho	9.9204(21)	7.4543(16)	4.8107(10)	91°21.4'(1')	18.6	16.0(0.02,104)
Er	9.9025(18)	7.4200(13)	4.7943(8)	91°14.3'(1')	21.9	17.4(0.02,106)
Y	9.9213(15)	7.4431(12)	4.8093(7)	91°17.5'(0.7')	21.8	20.9(0.015,112)

* No extinction rule has been used for calculating F_N ; F_N has been calculated for the CoKα radiation.

TABLE 4.

VIBRATIONAL SPECTRUM OF $LaBGeO_5$.

INFRARED		RAMAN	
^{10}B *	^{n}B *	^{10}B	^{n}B
1115	1087		
1012	988		
975	960		
935	920		
875	858	863	861
862	850		
828	826	828	825
		802	802
792	790		
738	735		
700	696	703	700
		632	631
616	616		
553	549	555	550
500	500	500	499
427	427	425	425
388	388	388	388
≈375	≈375	≈372	≈372
342	342		
		337	337
307	307	308	308
		300	300
		273	273
262	262	261	261
232	233	232	232
		205	205
197	196		
177	177		
		162	162
		142	142
		123	123
120	119		
		108	107
		92	91
88	88		

* ^{10}B stands for an isotopic composition with 92.4 % ^{10}B
^{n}B is the natural isotopic composition (81.17 % ^{11}B).

TABLE 5.

VIBRATIONAL SPECTRUM OF $GdBGeO_5$.

INFRARED		RAMAN	
^{10}B	^{n}B	^{10}B	^{n}B
1155	1120		
1021	1000	974	958
	950		
943	939		
		931	930
		853	853
806	804		
775	770	762	771
	760		
694	689		
		675	675
670	668		
568	567	567	567
		513	509
	505		
490	490	438	438
431	430	426	426
		404	403
		393	392
374	373		
350	350	335	336
310	310	294	295
	277	274	275
			252
			245
	236		
	225		225
			216
	205		200
			177
			166
	155		155
			138
	120		122
			110
			97
			84

LEGENDS OF THE FIGURES.

Fig. 1 : Relationship between the unit cell parameters and the ionic radius of Ln for the monoclinic phases. The ionic radii are those of Shannon (9) for an eightfold coordination of Ln.

Fig. 2 : IR spectra of $LaBGeO_5$ and $LaBSiO_5$.

Fig. 3 : Raman spectra of $LaBGeO_5$ and $LaBSiO_5$.

Fig. 4 : Raman and IR spectra of $GdBGeO_5$.

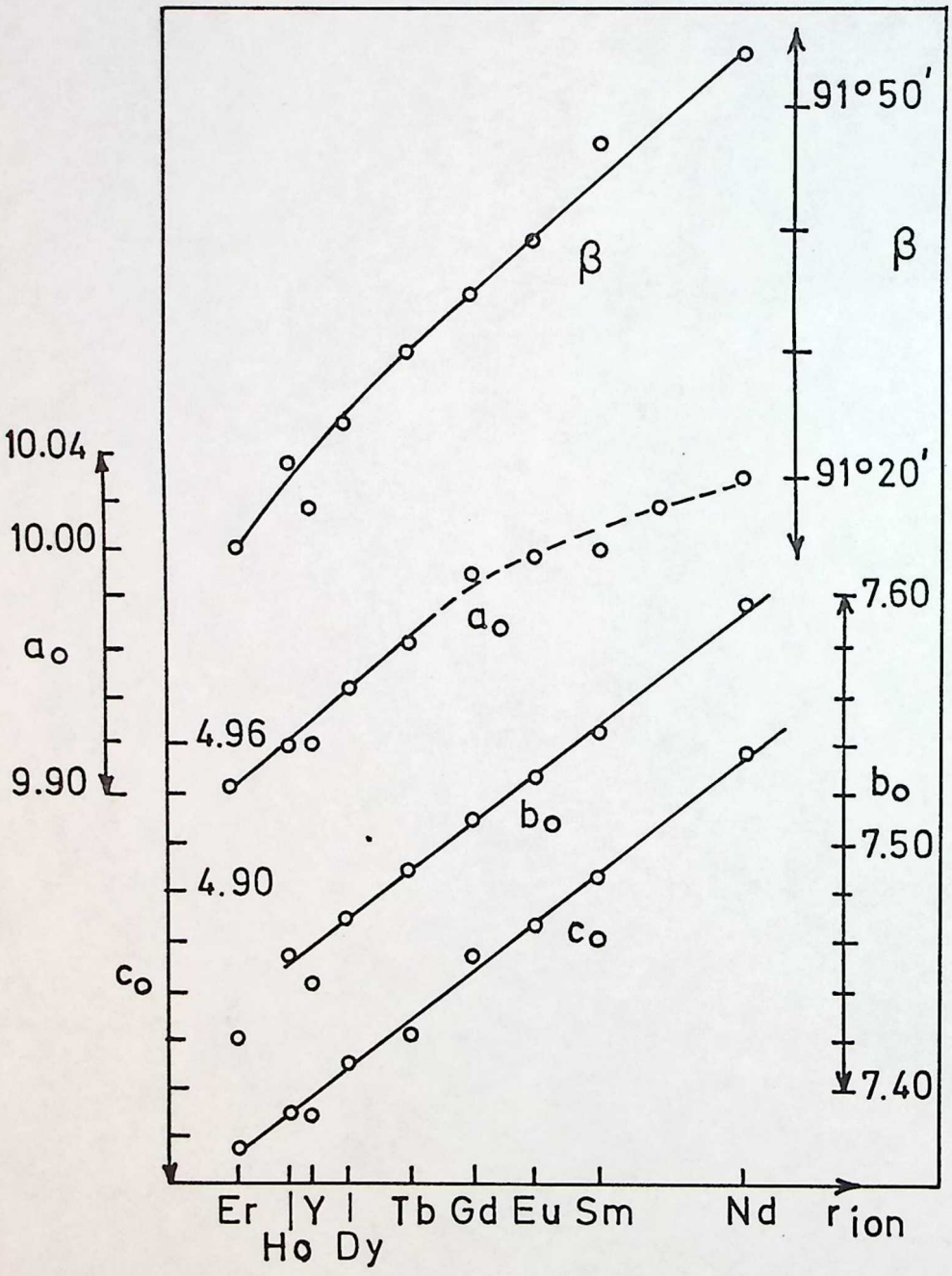
91°50'
β
β
91°20'
10.04
10.00
a_o
9.90
a_o
4.96
7.60
b_o
7.50
b_o
4.90
c_o
c_o
7.40
Er
Ho
Y
Dy
Tb
Gd
Eu
Sm
Nd
r_{ion}

Fig. 1

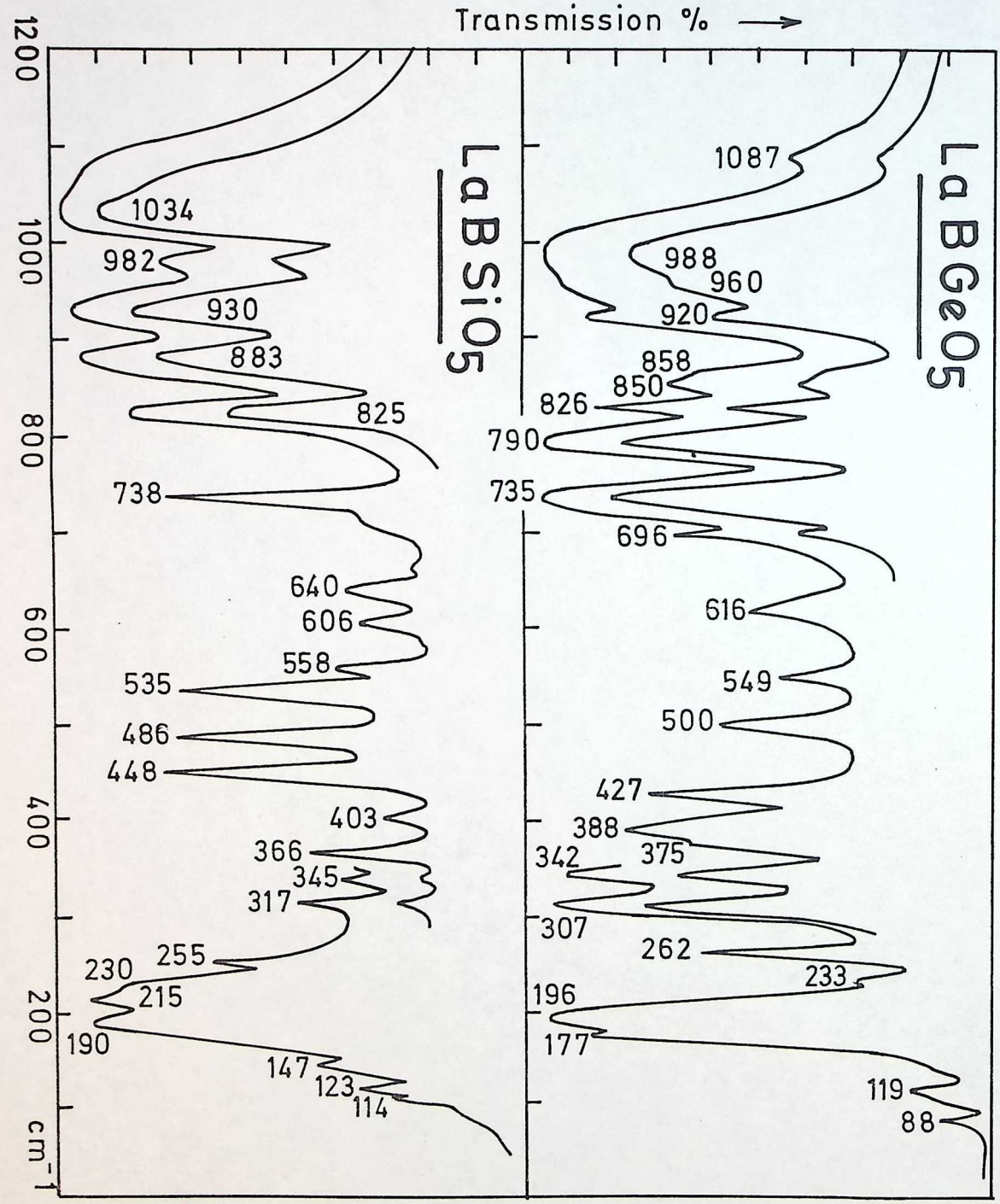
Transmission % →
LaBSiO5
1034
982
930
883
825
738
640
606
558
535
486
448
403
366
345
317
255
230
215
190
147
123
114
LaBGeO5
1087
988
960
920
858
850
826
790
735
696
616
549
500
427
388
375
342
307
262
233
196
177
119
88
1200
1000
800
600
400
200
cm⁻¹

Fig. 2

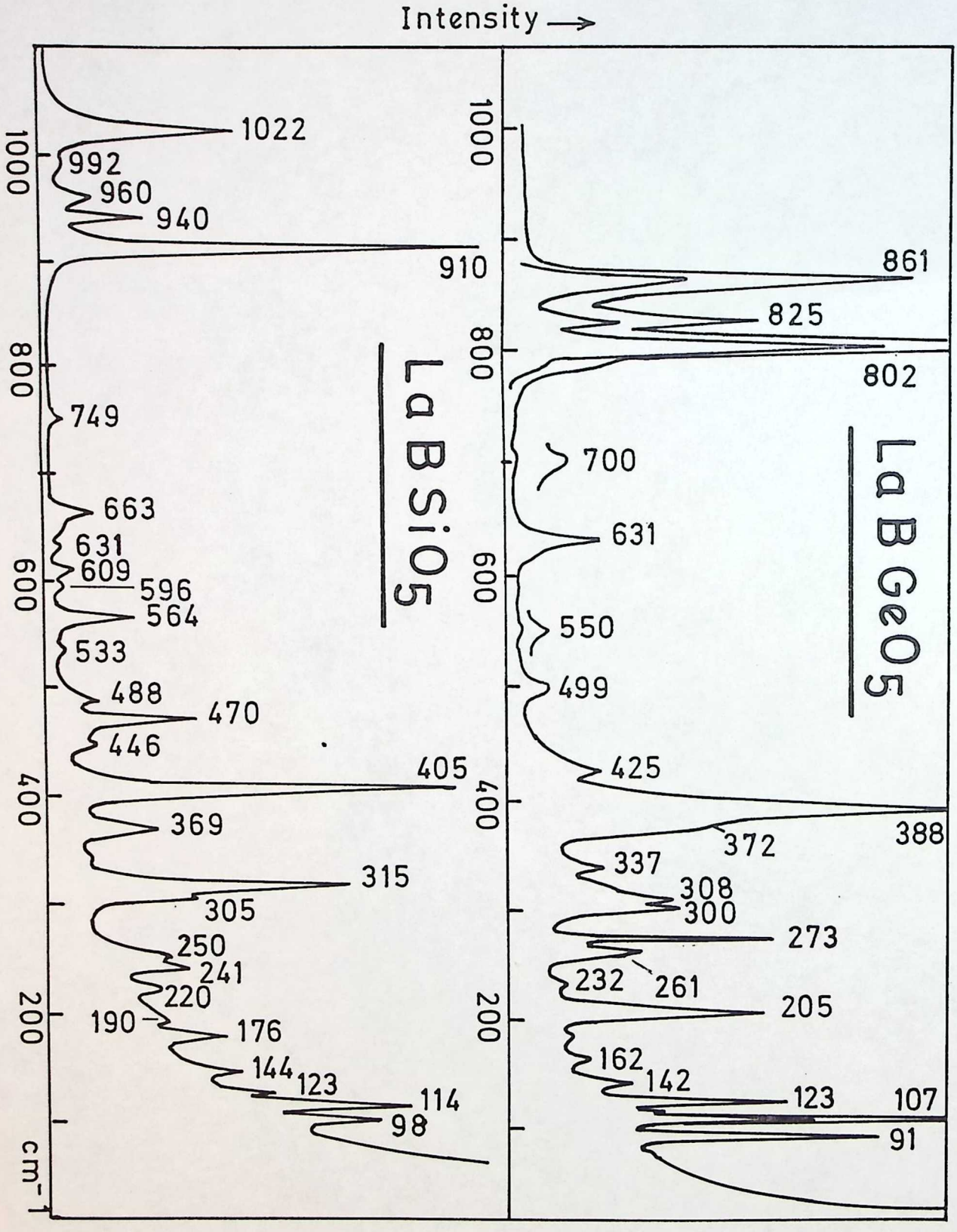
Intensity →
LaBSiO5
1022
992
960
940
910
749
663
631
609
596
564
533
488
470
446
405
369
315
305
250
241
220
190
176
144
123
114
98
LaBGeO5
861
825
802
700
631
550
499
425
388
372
337
308
300
273
232
261
205
162
142
123
107
91
1000
800
600
400
200
cm⁻¹

Fig. 3

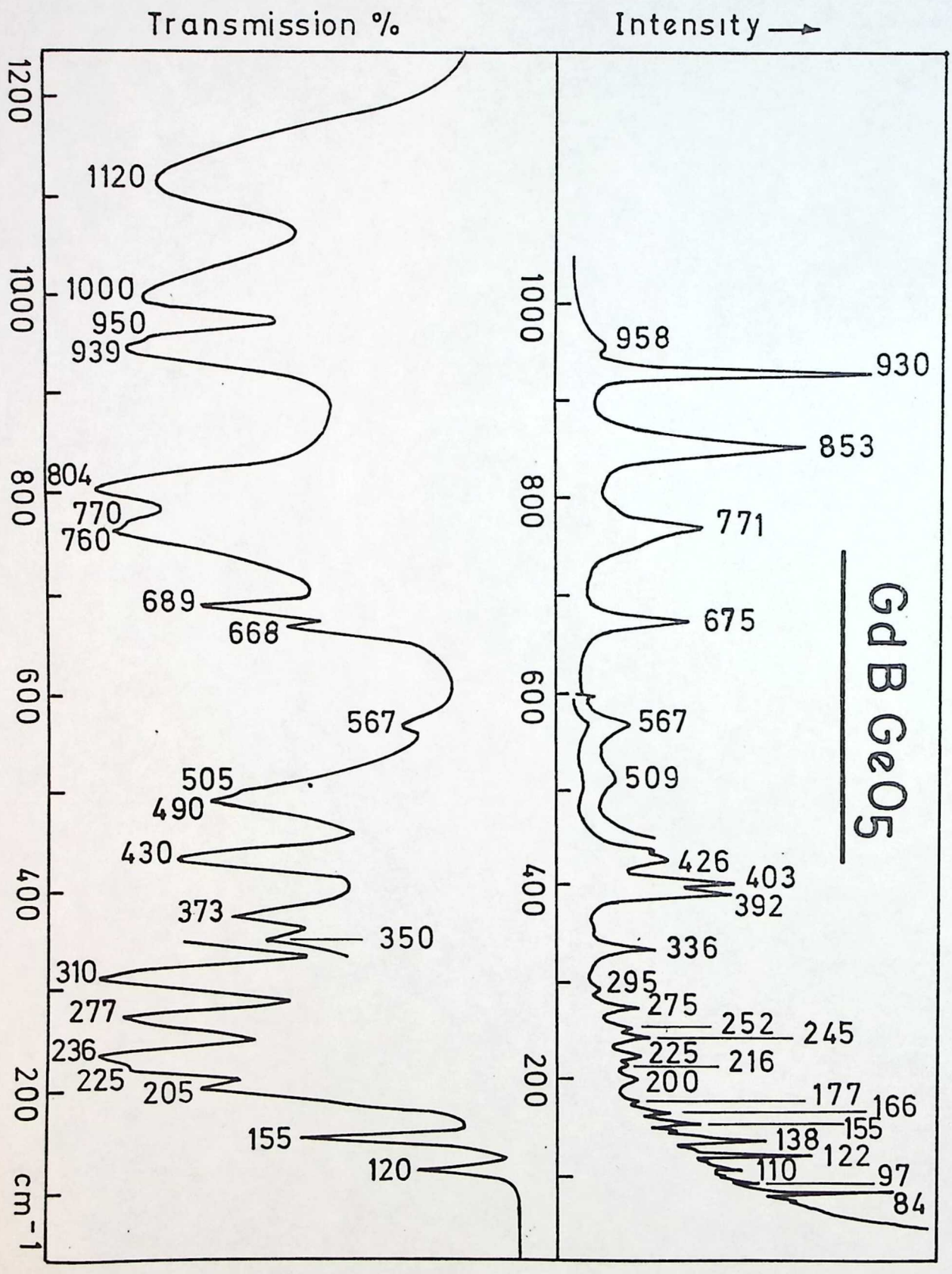
Transmission %
Intensity
1200
1000
800
600
400
200
cm⁻¹
1120
1000
950
939
804
770
760
689
668
567
505
490
430
373
350
310
277
236
225
205
155
120
958
930
853
771
675
567
509
426
403
392
336
295
275
252
245
225
216
200
177
166
155
138
122
110
97
84
GdBGeO5

Fig. 4